Short communication

Synthesis and characterization of $LiCo_{1/3}Mn_{1/3}Fe_{1/3}PO_4$/C nanocomposite cathode of lithium batteries with high rate performance

CrossMark

Sou Akimoto, Izumi Taniguchi*

Department of Chemical Engineering, Graduate School of Science and Engineering, Tokyo Institute of Technology, 12-1, Ookayama-2, Meguro-ku, Tokyo 152-8552, Japan

HIGHLIGHTS

- $LiCo_{1/3}Mn_{1/3}Fe_{1/3}PO_4$ nanocomposites were prepared by a novel preparation route.
- $LiCo_{1/3}Mn_{1/3}Fe_{1/3}PO_4$/C nanocomposites were agglomerates of primary particles.
- The carbon was well distributed on the surface of agglomerates.
- The nanocomposite cathode delivered a discharge capacity of 159 mAh g^{-1} at 0.05 C.
- The nanocomposite cathode showed good cycle and high-rate performance.

ARTICLE INFO

ABSTRACT

Olivine structured $LiCo_{1/3}Mn_{1/3}Fe_{1/3}PO_4$/C nanocomposites were prepared by a combination of spray pyrolysis at 300 °C and wet ball-milling followed by heat treatment at 500 °C for 4 h in a 3%H_2 + N_2 atmosphere. The formation of a solid solution between $LiCoPO_4$, $LiMnPO_4$, and $LiFePO_4$ at this composition was confirmed by X-ray diffraction analysis. Scanning electron microscopy and transmission electron microscopy with equipped energy dispersive spectroscopy verified that the $LiCo_{1/3}Mn_{1/3}Fe_{1/3}PO_4$/C nanocomposites were agglomerates of $LiCo_{1/3}Mn_{1/3}Fe_{1/3}PO_4$ primary particles with a geometric mean diameter of 107 nm and a uniform chemical composition, and carbon was well distributed on the surface of the agglomerates. The $LiCo_{1/3}Mn_{1/3}Fe_{1/3}PO_4$/C nanocomposite cathode exhibited a high discharge capacity of 159 mAh g^{-1} at 0.05 C in the potential range of 2.0–5.0 V, corresponding to 94% of theoretical capacity. The capacity retention was 87% after 50 cycles at a charge–discharge rate of 1 C. Furthermore, the rate capability test showed that the high capacity still was retained even at 5 C and 20 C rate with 106 and 72 mAh g^{-1}, respectively.

1. Introduction

The successful development of $LiFePO_4$ as a cathode active material for lithium-ion batteries has promoted strong interest in other transition metal phosphates such as $LiMnPO_4$ and $LiCoPO_4$. Although $LiFePO_4$ is low cost, stable and has excellent battery performance due to mix with carbon, its working voltage is restricted to approximately 3.5 V versus Li/Li$^+$ [1]. In comparison with $LiFePO_4$, $LiMnPO_4$ and $LiCoPO_4$ present much higher redox potentials (4.1 V [1] and 4.8 V [2] versus Li/Li$^+$, respectively) and have almost the same theoretical capacity of approximately 170 mAh g^{-1}. As a result, the theoretical energy density is significantly larger than that of $LiFePO_4$. However, a few reports have been done for the $LiMnPO_4$ and $LiCoPO_4$ cathodes with good electrochemical properties [3–5]. Recently, olivine solid solutions such as $LiFe_{1-x}Mn_xPO_4$ [6], $LiFe_{1-x}Co_xPO_4$ [7], $LiCo_{1/3}Mn_{1/3}Fe_{1/3}PO_4$ [8–12] and $LiMn_{1-x}Co_xPO_4$ [13,14] have also been investigated to overcome this problem. However, the practical application of them still requires to improve the electrochemical properties.

Recently, we have developed a novel preparation method for $LiMPO_4$/C (M = Fe, Mn and Co) nanocomposites [15–19] to improve their electrochemical performance. In this paper, we report the synthesis of $LiCo_{1/3}Mn_{1/3}Fe_{1/3}PO_4$/C nanocomposites by the novel

* Corresponding author. Tel./fax: +81 3 5734 2155.
E-mail addresses: taniguchi.i.aa@m.titech.ac.jp, itaniguc@chemeng.titech.ac.jp (I. Taniguchi).

preparation method and its electrochemical performance in galvanostatic charge–discharge tests.

2. Experimental

$LiCo_{1/3}Mn_{1/3}Fe_{1/3}PO_4$ precursors were prepared by spray pyrolysis at 300 °C. A schematic diagram of the spray pyrolysis apparatus used has been provided elsewhere [20]. The precursor solution was prepared by dissolving the required amounts of $LiNO_3$ (98% purity), H_3PO_4 (85% purity), $Co(NO_3)_2 \cdot 6H_2O$ (98% purity), $Mn(NO_3)_2 \cdot 6H_2O$ (98% purity) and $Fe(NO_3)_3 \cdot 9H_2O$ (98% purity) in distilled water in stoichiometric ratios. It was atomized at a frequency of 1.7 MHz using an ultrasonic nebulizer. The generated droplets were carried to a reactor furnace by a $N_2 + 3\%H_2$ carrier gas medium. The $LiCo_{1/3}Mn_{1/3}Fe_{1/3}PO_4$ precursors obtained in the reactor exit were collected using an electrostatic precipitator, which operated at 180 °C, to prevent the condensation of vapor on the precursors. The reactor temperature was 300 °C and the gas flow rate was fixed at 2 dm^3 min^{-1}. The $LiCo_{1/3}Mn_{1/3}Fe_{1/3}PO_4$ precursors were milled with 10 wt.% of acetylene black in ethanol by a planetary high-energy ball-milling (Fritsch, pulverisette 7) at 800 rpm for 6 h, and then annealed at 500 °C for 4 h in a $N_2 + 3\%H_2$ atmosphere.

The crystalline phases of the samples were studied by X-ray diffraction (XRD, Rigaku, Ultima IV with D/teX Ultra) analysis using Cu-Kα radiation. The lattice parameters of the materials were refined by Rietveld analysis using an integrated X-ray powder diffraction software package PDXL (Rigaku, Version 1.3.0.0). The surface morphology of the sample was examined by field emission scanning electron microscopy (FE-SEM, Hitachi, S4500) equipped with energy dispersive spectroscopy (EDS) operated at 8 kV. The interior structure of the sample was observed by using transmission electronic microscopy (TEM, JEOL, Ltd., JEM-2010F) with EDS.

The electrochemical performance of $LiCo_{1/3}Mn_{1/3}Fe_{1/3}PO_4$/C nanocomposites was investigated using coin-type cells (CR2032). The cell was composed of a lithium metal negative electrode and a $LiCo_{1/3}Mn_{1/3}Fe_{1/3}PO_4$/C composite positive electrode that were separated by a microporous polypropylene film. 1 mol dm^{-3} LiPF$_6$ solution in a solvent mixture of ethylene carbonate (EC) and dimethyl carbonate (DMC) with 1:1 in volume ratio (Tomiyama Pure Chemical Co., Ltd.) was used as the electrolyte. The cathode consisted of 70 wt.% $LiCo_{1/3}Mn_{1/3}Fe_{1/3}PO_4$, 10 wt.% polyvinylidene fluoride (PVdF) as a binder and 20 wt.% acetylene black, which included the acetylene black in the $LiCo_{1/3}Mn_{1/3}Fe_{1/3}PO_4$/C nanocomposites. The cells were tested galvanostatically between 2.0 and 5.0 V versus Li/Li$^+$ with multi-channel battery testers (Hokuto Denko, HJ1010mSM8A)
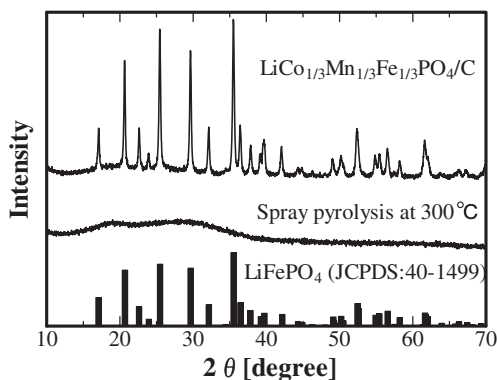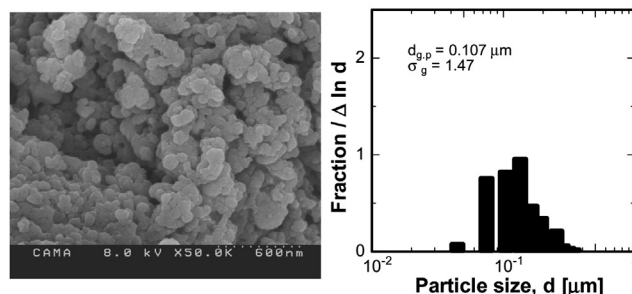
at various charge–discharge rates ranging from 0.05 to 20 C (1 C = 170 mAh g^{-1}). Current densities and specific capacities were calculated on the basis of the weight of $LiCo_{1/3}Mn_{1/3}Fe_{1/3}PO_4$ in the cathode. Cyclic voltammetry (CV) was measured at a scanning rate of 0.1 mV s^{-1} in a potential range of 2.0–5.0 V using the Solartron 1255B frequency response analyzer connected to a Solartron SI 1287 electrochemical interface. All electrochemical measurements were performed at room temperature.

3. Results and discussion

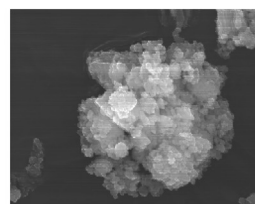### 3.1. Physical properties of $LiCo_{1/3}Mn_{1/3}Fe_{1/3}PO_4$/C nanocomposites

Fig. 1 shows the XRD patterns of the sample (a) synthesized by spray pyrolysis at 300 °C and the final sample (b) prepared by a combination of spray pyrolysis at 300 °C and wet ball-milling followed by heat treatment at 500 °C for 4 h in a $3\%H_2 + N_2$ atmosphere. The JCPDS card data of LiFePO$_4$ (JCPDS 40-1499) is also

Table 1
Lattice parameters of $LiCo_{1/3}Mn_{1/3}Fe_{1/3}PO_4$ and LiMPO$_4$ (M = Fe, Mn, or Co).

	a [Å]	b [Å]	c [Å]	V [Å^3]
$LiCo_{1/3}Mn_{1/3}Fe_{1/3}PO_4$/C (this work)	10.327	6.012	4.713	292.611
$LiCo_{1/3}Mn_{1/3}Fe_{1/3}PO_4$/C [10]	10.328	6.012	4.711	292.536
$LiCo_{1/3}Mn_{1/3}Fe_{1/3}PO_4$ [11]	10.326	6.011	4.713	292.534
$LiCo_{0.33}Mn_{0.33}Fe_{0.33}PO_4$ [12]	10.337	6.008	4.717	292.95
LiFePO$_4$ (JCPDS No. 40-1499)	10.347	6.019	4.704	292.959
LiMnPO$_4$ (JCPDS No. 33-0804)	10.454	6.106	4.749	303.139
LiCoPO$_4$ (JCPDS No. 32-0552)	10.206	5.922	4.701	284.128

(a) Morphology and primary particle size distribution

(b) Element mapping

Fig. 1. XRD patterns of the sample (a) synthesized by spray pyrolysis at 300 °C and the final sample (b) prepared by a combination of spray pyrolysis at 300 °C and wet ball-milling followed by heat treatment at 500 °C for 4 h in a $3\%H_2 + N_2$ atmosphere.
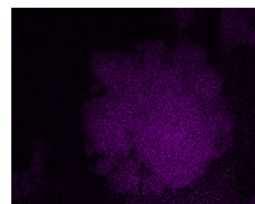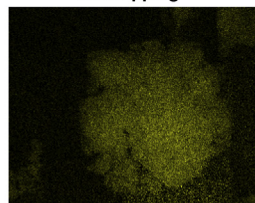
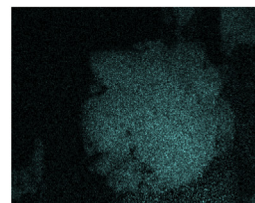**Fig. 2.** SEM images and element mapping of the $LiCo_{1/3}Mn_{1/3}Fe_{1/3}PO_4$/C nanocomposites.

shown in the figure as the reference. There is no diffraction peak in the XRD patterns of the sample prepared by spray pyrolysis at 300 °C. On the other hand, the final sample shows the single phase that can be indexed on the orthorhombic structure with a space group Pnmb. The diffraction peaks of final sample are also similar to those of $LiFePO_4$ single phase, but the peak locations change slightly [9]. Lattice parameters of the $LiCo_{1/3}Mn_{1/3}Fe_{1/3}PO_4/C$ composites obtained from Rietveld refinement are summarized in Table 1. All the values are in good agreement with the reported data [10–12]. The lattice parameters of $LiCo_{1/3}Mn_{1/3}Fe_{1/3}PO_4/C$ closely follow the average values of the radius of transition-metal ion, Co^{2+} (0.72 Å), Mn^{2+} (0.84 Å), and Fe^{2+} (0.74 Å) in the phosphates. From the above mentioned results, the complete solid solution among $LiMnPO_4$, $LiFePO_4$, and $LiCoPO_4$ could be confirmed in the final sample.

The morphology, particle size distribution and EDS mapping results for the $LiCo_{1/3}Mn_{1/3}Fe_{1/3}PO_4/C$ composites are shown in Fig. 2. It is obvious in Fig. 2a that the $LiCo_{1/3}Mn_{1/3}Fe_{1/3}PO_4/C$ composites are the agglomerates of primary particles with a geometric mean diameter of 107 nm. From the EDS mapping results (Fig. 2b), it is clearly observed that Co, Mn and Fe were uniformly distributed in the $LiCo_{1/3}Mn_{1/3}Fe_{1/3}PO_4/C$ composites. This observation confirms that $LiCo_{1/3}Mn_{1/3}Fe_{1/3}PO_4/C$ composites with a homogeneous chemical composition can be prepared via the present preparation method. The distribution of carbon in the $LiCo_{1/3}Mn_{1/3}Fe_{1/3}PO_4/C$ composites was investigated by TEM and EDS. The obtained results are shown in Fig. 3. The TEM and EDS observations reveal that the agglomerates of $LiCo_{1/3}Mn_{1/3}Fe_{1/3}PO_4$ nanoparticles are uniformly covered by a thin carbon layer with a thickness on the order of 10 nm. As a result, these characterizations lead to the conclusion that the $LiCo_{1/3}Mn_{1/3}Fe_{1/3}PO_4/C$ nanocomposites could be successfully synthesized by the combination of spray pyrolysis and wet ball-milling followed by heat treatment.

3.2. Electrochemical performance of $LiCo_{1/3}Mn_{1/3}Fe_{1/3}PO_4/C$ nanocomposites

The initial galvanostatic charge and discharge curves for $Li/LiCo_{1/3}Mn_{1/3}Fe_{1/3}PO_4/C$ nanocomposite test cell are shown in Fig. 4a, measured at a charge–discharge rate of 0.05 C in the potential range of 2.0–5.0 V. Three characteristic potential plateaus associating with Fe, Mn and Co appear clearly in both charge and discharge curves. The first potential plateau at approximately 3.5 V is attributed to the redox process of Fe^{2+}/Fe^{3+}, the second one close to 4.2 V is related to the redox process of Mn^{3+}/Mn^{2+} and the 3rd one near 4.8 V is associated with the redox process of Co^{3+}/Co^{2+}. The indication of redox couples for each potential plateau has been also confirmed by the CV measurements of the test cell, as shown in Fig. 4b. These facts may indicate the $LiCo_{1/3}Mn_{1/3}Fe_{1/3}PO_4$ with a well-ordered olivine structure could be obtained by the present method. Also, the cell delivers a first discharge capacity of
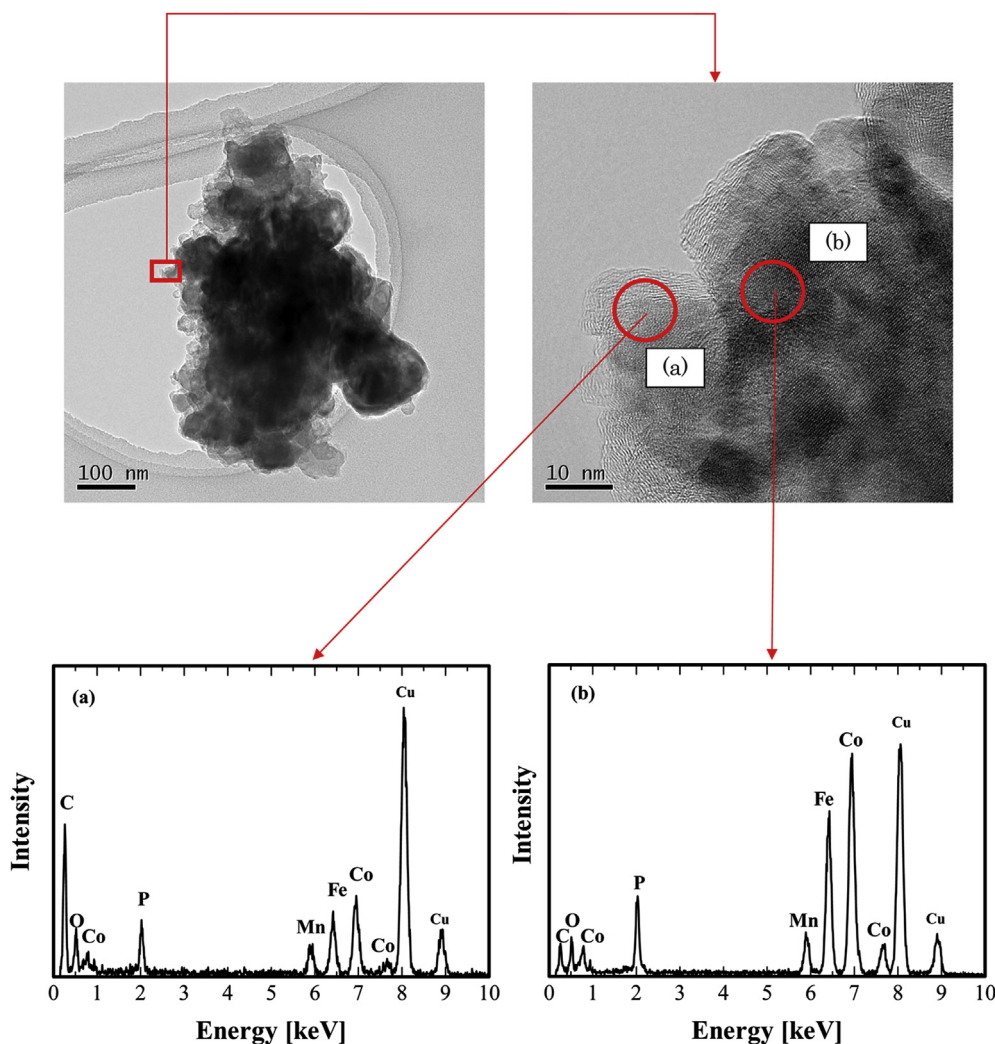

Fig. 3. TEM images and EDS spectrum of the $LiCo_{1/3}Mn_{1/3}Fe_{1/3}PO_4/C$ nanocomposites.

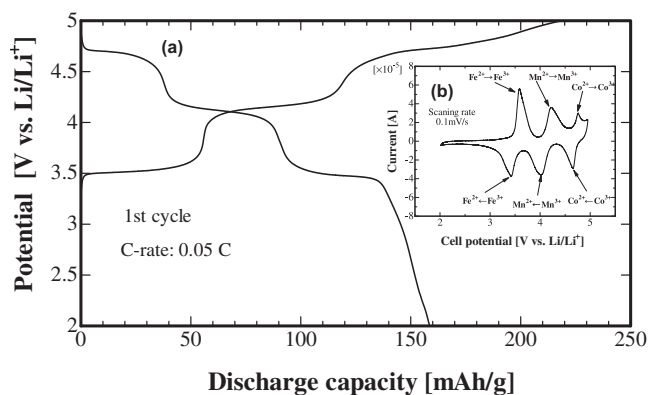**Fig. 4.** First charge and discharge curves (a) and CV (b) of the $LiCo_{1/3}Mn_{1/3}Co_{1/3}PO_4/C$ nanocomposites.

159 mAh g^{-1}, corresponding to 94% of its theoretical capacity, and the average potential rose up to 3.88 V owing to the incorporation of Mn and Co.

Fig. 5a shows the electrochemical performance of Li/$LiCo_{1/3}Mn_{1/3}Fe_{1/3}PO_4$/C nanocomposite test cell at various charge–discharge rates ranging from 0.05 to 20 C. The cell exhibits first discharge capacities of 159 mAh g^{-1} at 0.05 C, 143 mAh g^{-1} at 1 C, 106 mAh g^{-1} at 5 C and 72 mAh g^{-1} at 20 C. Moreover, three distinct potential plateaus in the discharge profile exist clearly up to a charge–discharge rate of 5 C, and they still retain even at a charge–discharge rate of 20 C. As a result, the cell showed a superior rate capability. The cycle performance of Li/$LiCo_{1/3}Mn_{1/3}Fe_{1/3}PO_4$/C nanocomposite test cell was shown in Fig. 5b. The cell was charged and discharge at 1 C rate. For comparison, the reported cycle performance data for LiMnPO$_4$/C [17] and LiCoPO$_4$/C [19]
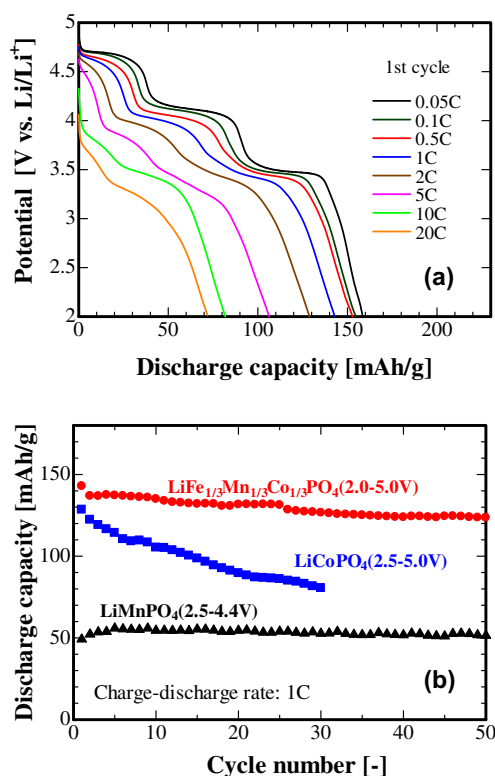
nanocomposites were also plotted in the figure. The first discharge capacity is 143 mAh g^{-1}, and the capacity retention based on the first discharge capacity is 87% after 50 cycles. Thus far, the large capacity fading of LiCoPO$_4$/C and the low rate capability of LiMnPO$_4$/C are reported in the literature [16,18,19,21,22]. The Li/$LiCo_{1/3}Mn_{1/3}Fe_{1/3}PO_4$/C nanocomposite cell shows a good cycle and high rate performance. These may be due to the small primary particles, homogeneous chemical composition and a well distributed carbon in the $LiCo_{1/3}Mn_{1/3}Fe_{1/3}PO_4$/C nanocomposites. Furthermore, the enhanced ionic conductivity and the reduced high working potential regime of the sample owing to the partially replacement of Fe and Co for Mn in LiMnPO$_4$ might also lead to improve the electrochemical activities of the sample.

4. Conclusions

$LiCo_{1/3}Mn_{1/3}Fe_{1/3}PO_4$/C nanocomposites were successfully prepared via the combination of spray pyrolysis at 300 °C and wet ball-milling followed by heat treatment at 500 °C for 4 h in a 3%H$_2$ + N$_2$ atmosphere. The XRD patterns of the $LiCo_{1/3}Mn_{1/3}Fe_{1/3}PO_4$/C nanocomposites could be identified as a single phase of olivine structure indexed by orthorhombic *Pmna*. The calculated lattice parameters were well agreed with the reported data. The $LiCo_{1/3}Mn_{1/3}Fe_{1/3}PO_4$/C nanocomposites were agglomerates with a homogeneous chemical composition, which comprised of $LiCo_{1/3}Mn_{1/3}Fe_{1/3}PO_4$ primary particles with a geometric mean diameter of 104 nm and were uniformly covered by a thin carbon layer with a thickness on the order of 10 nm.

The obtained $LiCo_{1/3}Mn_{1/3}Fe_{1/3}PO_4$/C nanocomposite cathode exhibited excellent electrochemical performance. The first discharge capacity was 159 mAh g^{-1} at a charge–discharge rate of 0.05 C, corresponding to 94% of its theoretical capacity. The capacity retention based on the first discharge capacity is 87% after 50 cycles at a charge–discharge rate of 1 C. Moreover, the high discharge capacity still remained even at charge–discharge rates of 5 C and 20 C with 106 and 72 mAh g^{-1}, respectively. The superior electrochemical performance may be attributed to the small primary particles, homogeneous chemical composition and well distributed carbons in the $LiCo_{1/3}Mn_{1/3}Fe_{1/3}PO_4$/C nanocomposite cathode.

Fig. 5. Rate capability (a) and cyclability (b) of the $LiCo_{1/3}Mn_{1/3}Co_{1/3}PO_4$/C nanocomposites.

References

[1] A.K. Padhi, K.S. Nanjundaswamy, J.B. Goodenough, J. Electrochem. Soc. 144 (1997) 1188–1194.
[2] A. Amine, H. Yasuda, M. Yamachi, Electrochem. Solid State Lett. 3 (2003) 178–179.
[3] L. Su, Y. Jing, Z. Zhou, Nanoscale 3 (2011) 3967–3983.
[4] L.Y. Xing, M. Hu, Q. Tang, J.P. Wei, X. Qin, Z. Zhou, Electrochim. Acta 59 (2012) 172–178.
[5] M. Hu, X. Pang, Z. Zhou, J. Power Sources 237 (2013) 229–242.
[6] J. Molenda, W. Ojczyk, J. Marzec, J. Power Sources 174 (2007) 689–694.
[7] D. Wang, Z. Wang, X. Huang, L. Chen, J. Power Sources 146 (2005) 580–583.
[8] Y.-C. Chen, J.-M. Chen, C.-H. Hsu, J.-J. Lee, T.-C. Lin, J.-W. Yeh, H.C. Shih, J. Power Sources 195 (2010) 6867–6872.
[9] H. Gwon, D.-H. Seo, S.-W. Kim, J. Kim, K. Kang, Adv. Funct. Mater. 19 (2009) 3285–3292.
[10] Y. Zhang, C.S. Sun, Z. Zhou, Electrochem. Commun. 11 (2009) 1183–1186.
[11] Y.-U. Park, J. Kim, H. Gwon, D.-H. Seo, S.-W. Kim, K. Kang, Chem. Mater. 22 (2010) 2573–2581.
[12] J. Chen, M.J. Vacchio, S. Wang, N. Chernova, P.Y. Zavalij, M.S. Whittingham, Solid State Ion. 178 (2008) 1676–1693.
[13] I. Taniguchi, T.N.L. Doan, B. Shao, Electrochim. Acta 56 (2011) 7680–7685.
[14] J.F. Ni, Y. Han, J. Liu, H. Wang, L. Gao, ECS Electrochem. Lett. 2 (2013) A3–A5.
[15] M. Konarova, I. Taniguchi, J. Power Sources 195 (2010) 3661–3667.
[16] Z. Bakenov, I. Taniguchi, Electrochem. Commun. 12 (2010) 75–78.
[17] T.N.L. Doan, I. Taniguchi, J. Power Sources 196 (2011) 1399–1408.
[18] T.N.L. Doan, I. Taniguchi, J. Power Sources 196 (2011) 5679–5684.
[19] T.N.L. Doan, I. Taniguchi, Powder Technol. 217 (2012) 574–580.
[20] I. Taniguchi, Mater. Chem. Phys. 92 (2005) 172–179.
[21] H.H. Li, J. Jin, J.P. Wei, Z. Zhou, J. Yan, Electrochem. Commun. 11 (2009) 95–98.
[22] L. Damen, F.D. Giorgio, S. Monaco, F. Veronesi, M. Mastragostino, J. Power Sources 218 (2012) 250–253.